Applied Thermal Engineering 292 (2026) 130257

Contents lists available at ScienceDirect

Applied Thermal Engineering

journal homepage: www.elsevier.com/locate/apthermeng

Research Paper

Enhancing the efficiency of solar photovoltaic systems via smart cooling in arid environments

Zineb Chaich [a], Djamel Belatrache [b], Lazhar Labiod [c], Mahmoud Bourouis [d,*]

[a] Kasdi Merbah University, Department of Drilling and Oil Field Mechanics, 30000 Ouargla, Algeria
[b] Kasdi Merbah University, Department of Renewable Energies, VPRS Laboratory, 30000 Ouargla, Algeria
[c] Université de Paris, CNRS, Centre Borelli UMR 9010, F-75006 Paris, France
[d] Universitat Rovira i Virgili, Department of Mechanical Engineering, Av. Països Catalans 26, 43007 Tarragona, Spain

ARTICLE INFO

Keywords:
Photovoltaic panel
Smart cooling
Efficiency improvement
Water spraying system
Desert climate

ABSTRACT

Arid regions offer significant potential for photovoltaic (PV) energy generation due to their consistently high solar irradiance. However, the elevated operating temperatures common in such environments substantially reduce electrical efficiency and accelerate module degradation. This study presents an experimental investigation of a novel water-spray cooling system for active front-surface cooling of PV panels, with an emphasis on optimizing both thermal dissipation and water consumption.

The system consists of a top-mounted manifold with fine nozzles, powered by a pump and controlled by an Arduino-based unit that activates spraying only when module temperature exceeds a predefined threshold—an approach termed "smart cooling". A comparative outdoor experiment was conducted in Ouargla, Algeria, from June 9 to July 4, 2024, using two identical 390 W monocrystalline silicon panels: one equipped with the cooling system and one serving as an uncooled reference.

Under peak irradiance (979 W/m^2) and an ambient temperature of 40.4 °C, the cooled panel generated 350.5 W, compared with 272.1 W from the reference panel. This corresponds to a maximum efficiency gain of 28.8%, achieved as the surface temperature dropped from 58.6 °C to 36.7 °C. Continuous cooling improved average efficiency by 15.4%, whereas smart cooling delivered a comparable 15.5% improvement while using 84% less water. Additionally, the periodic spraying helped mitigate dust accumulation on the panel surface.

An economic analysis revealed that smart cooling lowers the annual levelized cost of power production to 0.07020 €/W, compared with 0.07514 €/W for continuous cooling and 0.07135 €/W for an uncooled module. These results demonstrate that adaptive water spraying can effectively enhance PV performance in arid climates while significantly conserving water resources.

1. Introduction

In recent years, developing countries have experienced a significant increase in energy demand due to rapid population growth and economic progress. This rising demand has resulted in a heavy dependency on conventional energy sources, contributing to severe environmental challenges such as greenhouse gas emissions and climate change. To address these issues, many governments have turned to sustainable energy strategies, focusing on integrating alternative sources like solar, wind, and hydroelectric power.

Algeria, with its excellent solar potential, has initiated numerous initiatives to develop solar energy as a vital energy vector of its energy policy. However, the efficiency of PV systems in the south region is significantly reduced by environmental conditions, particularly high temperatures and sand building on panel surfaces, which obstruct sunlight, further limiting energy output. Chaich et al. [1] examined the effects of dust collection and weather conditions on PV panels in southern Algeria, and they found that after three months of exposure, efficiency decreased by an average of 36.32%. Extreme weather conditions lead to a significant drop in the efficiency of PV modules. These problems underline the importance of cleaning and cooling the PV panels to enhance the performance. Finding solutions to these problems is vital to ensure that solar energy remains a viable and sustainable energy source for Algeria's future energy policy.

Recent investigations on PV cooling technologies have focused on integrating phase change materials (PCMs) to optimize heat dissipation and then enhance efficiency. Marudaipillai et al. [2] investigated a PCM

* Corresponding author.
E-mail address: mahmoud.bourouis@urv.cat (M. Bourouis).

https://doi.org/10.1016/j.applthermaleng.2026.130257
Received 25 November 2025; Received in revised form 4 February 2026; Accepted 11 February 2026
Available online 18 February 2026

Nomenclature

AMC	Annual operating and maintenance cost (€)
AP	Annual power productivity (W)
APC	Annual pump energy cost
ASV	Annual salvage value (€)
Ce	Electricity price (€/Kwh)
CPW	Annual cost per 1 W of power supply (€/W)
CS	Capital cost ($)
CRF	Capital recovery factor
FAC	Fixed annual cost (€)
i	Interest per year (%)
Imax	Maximum Current (A)
n	life time (year)
Pmax	Maximum power of PV module (W)

Subscripts

Amb	Ambient
A	cooled panel
B	reference panel
R	solar radiation (W/m^2)
S	area (m^2)
Sa	Salvage cost (€)
SFF	Sinking fund factor
T	Temperature (°C)
t	Time (Hour)
TAC	Total annual cost (€)
Vmax	Maximum voltage
U	Uncertainty
Xi	Independent variables
Z	Quantity of interest (dependent variable)

Greek letters

η	Efficiency (%)
η_{imp}	Efficiency improvement (%)

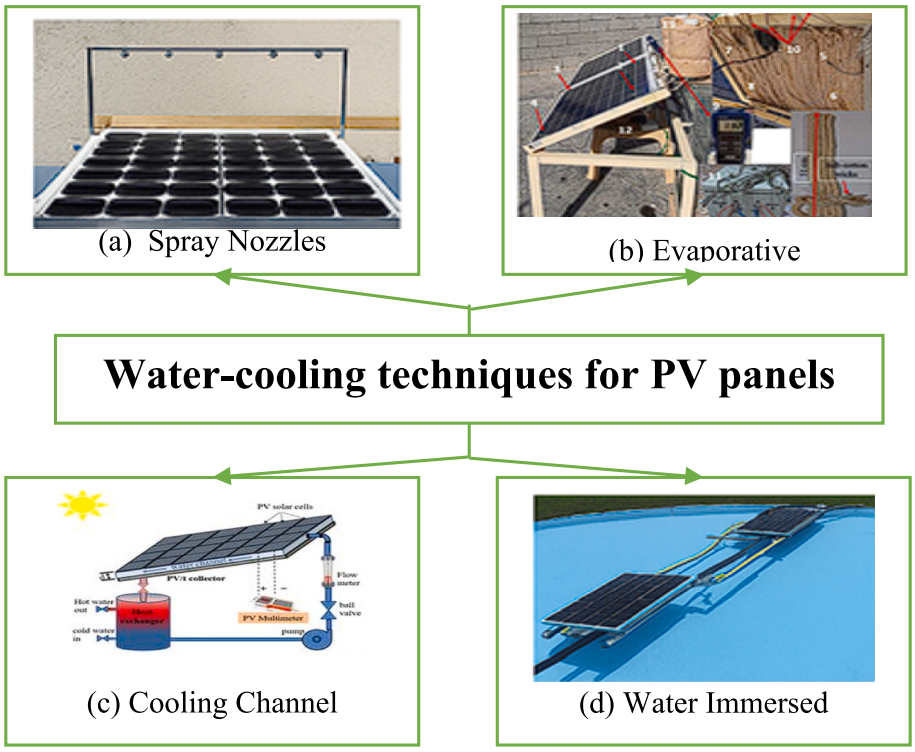

Fig. 1. Classification of the primary water-cooling methods. a) Spray Nozzles [12]. b) Evaporative [14]. (c) Cooling Channel [13]. (d) Water Immersed [11].

system composed of polyethylene glycol and expanded graphite, achieving a significant surface temperature reduction of 11.5 °C and increasing efficiency by 3.67%. Govindasamy and Kumar [3] explored three different phase change materials to determine the most effective method for enhancing solar panel efficiency. The best performance was obtained using paraffin and perlite, leading to a surface temperature reduction of 11 °C and an efficiency improvement by about3%. Zhenpeng et al. [4] reported that the PV-PCM system achieved a temperature drop of up to 23 °C, resulting in a 5.18% increase in electricity generation. Al Miaari and Ali [5] employed six small PCM-filled containers instead of a single large container. The average temperature decreased by around 10 °C, leading to a noticeable boost in energy output, approximately 5.23% more compared to modules without cooling.

Recent studies have explored air cooling methods, including fans and compressed air. Ahmed et al. [6] demonstrated that simple cooling with small fans increased efficiency by approximately 2.1%. Hernández et al. [7] tested forced air cooling with fans, which improved power output by 15%. King et al. [8] combined solar panels with a high-pressure compressed air system for cooling and dust removal. Their setup resulted in a significant performance boost, ranging from 7% to 12.6%. Nebbali et al. [9] attempted to channel ambient air to the back of the panels, achieving a 29.5-% increase in efficiency under harsh climatic conditions while reducing the panel temperature by 39.29 °C. Elminshawy et al. [10] found that directing cooled atmospheric air over the rear surface of photovoltaic panels lowered the module temperature from an average of 55 °C without cooling to 42 °C with an efficiency of about 23%.

Due to its high thermal capacity, water is an effective cooling method for PV systems, helping to reduce temperatures and enhance operational efficiency. Fig. 1 illustrates the classification of primary water-cooling methods. Spray nozzle cooling effectively dissipates heat and improves the performance of PV systems by directing water sprays onto the panels. Nižetić et al. [15] conducted an experimental study to evaluate the impact of water spraying on both the front and back surfaces of photovoltaic panels, finding that front surface cooling achieved an average efficiency of 15.4%. In comparison, back surface cooling reached 15.6%. Furthermore, the simultaneous cooling of both surfaces significantly reduced the panel temperature, lowering it from an average of 56 °C in the uncooled state to approximately 24 °C. Bevilacqua et al. [16] evaluated cooling using spray methods and forced ventilation applied to the rear surfaces of photovoltaic modules. The spray cooling system demonstrated superior performance, achieving an electrical efficiency of 14.3%, compared to 12.7% for the uncooled module. Laseinde et al. [17] investigated the optimization of a water spraying system, resulting in a 16.65% increase in efficiency. Zubeer et al. [18] carried out an experimental study to assess the combined influence of reflectors and water spray nozzle cooling on the performance of photovoltaic systems, finding that the integration of these two techniques led to a 17.7% increase. Raju et al. [19] examined the effect of front-surface water spraying on the performance of a mono-crystalline photovoltaic panel, revealing an enhancement of electrical efficiency of about 15.7% at a water flow rate of 170 L/h. Zubeer and Ali [20] utilized sunlight concentration (CPV) along with water cooling to enhance PV performance; the CPV system with cooling maintained lower temperatures (30–35 °C), increasing power output by 18.5%. Hassan et al. [21] combined numerical modeling and experimental investigations to assess the influence of various parameters on the heat transfer performance of PV/T systems. The configuration demonstrating the highest efficiency employed water in a tube with a diameter of 16 mm, resulting in an electrical efficiency of 14.8%. Bai et al. [22] found that applying water cooling to the top surface of a solar panel could reduce its temperature by up to 29.6 °C when comparing the maximum temperatures of cooled versus non-cooled cases. The average efficiency for the cooled panel was 1.94%, while the non-cooled panel showed 1.47%. Similarly, Hadipour et al. [23] used monocrystalline panels; the cooled panel exhibited a 33.3% increase in maximum electrical efficiency. Zhang et al. [24] found that under a spray pressure of 3 bars, the average cell temperature was 51.9 °C, and the conversion efficiency reached 17.58%, in contrast to 68.8 °C and 16.06% without spraying. Mostakim and Khodadad [25] employed a spray cooling system that resulted in a significant efficiency improvement of up to 16.78%, reducing the panel temperature from 45.08 °C to 34.12 °C.

Numerous experiments have been conducted to investigate the effectiveness of evaporative cooling solar panels. Yang et al. [27] developed a dew-point evaporative cooling system with two channels, maintaining over 15% efficiency and achieving a 16% gain compared to air cooling. According to the experimental findings by Chea et al. [28], evaporative cooling allowed the PV module temperature to drop by 15–23 °C while increasing the overall power output by over 15% compared to standard PV modules. Alktranee et al. [29] examined the effectiveness of two cooling techniques: rectangular aluminum fins and evaporative cooling. Their results showed that evaporative cooling not only reduced the temperature by 22.3% but also enhanced the output power of the photovoltaic module by as much as 21.3%. Baloch et al. [31] introduced a converging channel design to reduce and stabilize PV panel surface temperatures, leading to a temperature drop of up to 26 °C and improving the panel's conversion efficiency by 36.1%. Shalaby et al. [32] investigated the effect of cooling the back surface of polycrystalline PV panels using attached pipes, resulting in an increase in efficiency by 13.8%. Additionally, several studies have employed numerical simulations, validated by experimental data, to investigate PV and PVT module performance, including cooling strategies and nanofluid-enhanced heat transfer [33–35].

Table 1
Summary of the results from most studies on PV system cooling using water.

Authors	Type of PV Panel	Water Cooling Methods	Results
Nižetić et al. [15]	Monocrystalline	Spray	-Front surface cooling and rear surface cooling achieved an average efficiency of 15.4% and 15.6%, respectively. -Cooling of both surfaces reduced the panel temperature from an average of 56 °C to 24 °C.
Bevilacqua t al. [16]	Polycrystalline	Spray	An improvement in electrical efficiency of 14.3% was obtained, compared to 12.7% of the uncooled reference module.
Zubeer and Ali [18]	Polycrystalline	Spray	The temperature was reduced from 64.1 °C to 36.5 °C, resulting in an increase in electrical energy efficiency from 14.2% to 17%.
Raju et al. [19]	Monocrystalline	Spray	Electrical efficiency was improved by 15.7% at a water flow rate of 170 L/h.
Hadipour et al. [23]	Monocrystalline	Spray	The maximum electrical power output of the photovoltaic panel increased by about 33.3%.
Zhang et al. [24]	Polycrystalline	Spray	The PV cooling system reduced the cell temperature by an average of 12.3 °C and increased the conversion efficiency by an average of 1.1%.
Necib et al. [26]	Polycrystalline	Spray	The electrical efficiency of the PV panels increased from 17.6% without cooling to 21.9% with cooling.
Yang et al. [27]	Monocrystalline	Evaporative	Efficiency was increased by 16.4%.
Chea et al. [28]	Monocrystalline	Evaporative	-Drop of temperature by 15–23 °C while increasing the overall power output by over 15%.
Alktranee and Péter. [29]	Polycrystalline	Evaporative	-A reduction in temperature by 22.3%. -Enhancement of the output power by 21.3%.
Zhang et al. [30]	Monocrystalline	Cooling Channel	The total efficiency was improved by 18%.
Baloch et al. [31]	Monocrystalline	Cooling Channel	A temperature drop of up to 26 °C improved the panel's conversion efficiency by 36.1%.
Shalaby.et al. [32]	Polycrystalline	Cooling Channel	-The power generation was improved by about 14.1%. -The electrical efficiency reached 19.8% with cooling compared to 17.4% without cooling.
El Alami et al. [36]	Monocrystalline	Cooling Channel	The uncooled PV system experienced a cell temperature increase of **29.14** °C, whereas the cooled PVT system showed a rise of **7.04** °C, leading to electrical efficiency reductions of **1.98%** and **0.48%**, respectively
Saurabh Mehrotra et al. [37]	Monocrystalline	Water Immersed	Improvement in panel efficiency by 17.8% at a water depth of 1 cm.
Sivakumar et al. [38]	Polycrystalline	Water Immersed	Immersing the PV panel in 20 mm of tap water yielded

(*continued on next page*)

Table 1 (*continued*)

Authors	Type of PV Panel	Water Cooling Methods	Results
			the highest efficiency of 15.54%, resulting in a 9.1% improvement compared to the non-immersed panel.

Submerging photovoltaic panels in a water tank at a controlled depth provides an effective method for improving solar power generation, as shown in Fig. 1.d. Saurabh Mehrotra et al. [37] monitored the surface temperature of solar panels under high ambient temperature conditions. Their research revealed a 17.8% increase in panel efficiency with a water depth of 1 cm. Sivakumar et al. [38] investigated the effects of different immersion depths (10, 20, 30, and 40 mm) on PV panel electrical efficiency, yielding approximately 15.02%, 15.54%, 14.58%, and 13.95%, respectively. A summary of the effects and types of cooling for photovoltaic panels, based on various recent studies by PV type and efficiency, is presented in Table 1.

Algeria's vast desert regions, particularly Ouargla, are exposed to

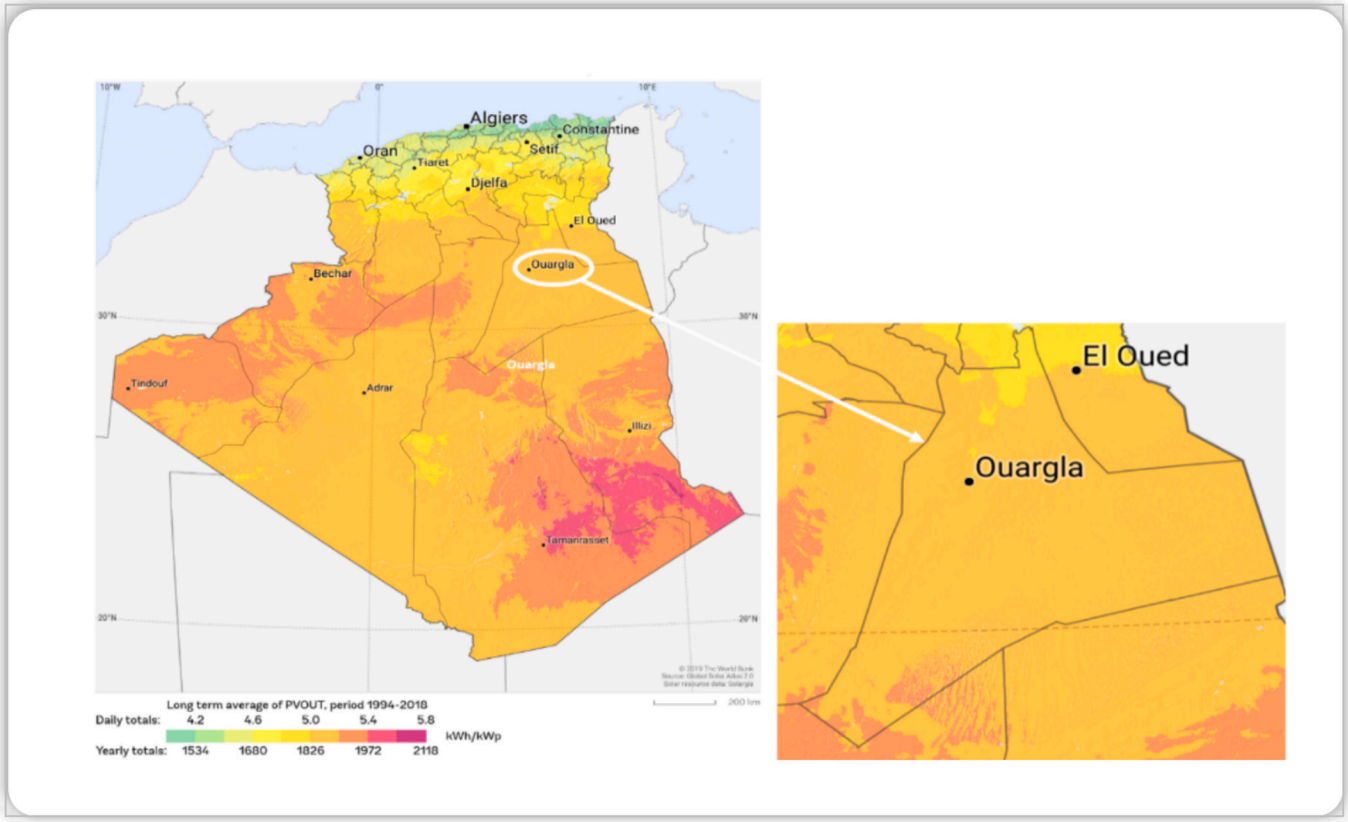

Fig. 2. PV power potential of the Ouargla region, Algeria [39].

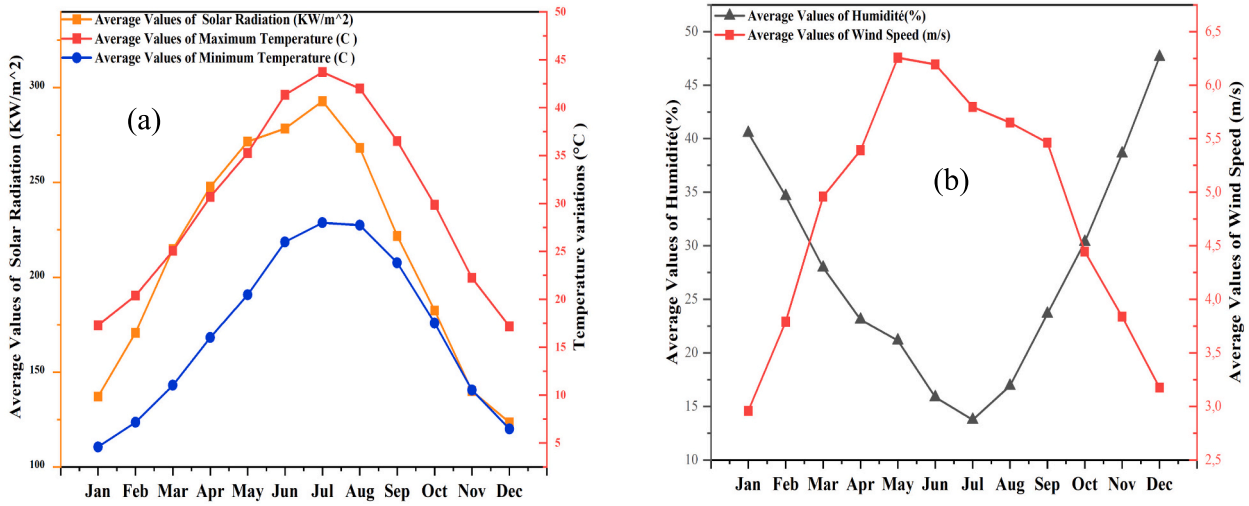

Fig. 3. Climatic Data for Ouargla City (2013–2023) [40].

Fig. 4. Schematic Diagram of the PV Panel Cooling System. (A) PVT panel, (B) PV panel, (1) water tank, (2) pump, (3) Pipe outlets, (4) Green Space and Grass, (5) Solar charge controller, (6) Battery, (7) Arduino with Relay, (8) Rheostat, (9) multimeter, (10) thermometer. (For interpretation of the references to colour in this figure legend, the reader is referred to the web version of this article.)

exceptionally high solar radiation and some of the highest ambient temperatures worldwide. These extreme conditions, characterized by high temperatures and low humidity, significantly reduce the efficiency and reliability of PV systems. Previous studies on PV cooling have largely focused on conventional techniques and have not fully addressed the combined challenges of desert climates and sustainable resource management.

The objective of this study is to experimentally develop and evaluate an eco-intelligent water-spraying cooling system designed to enhance the electrical performance of PV modules under harsh desert conditions. The system includes both continuous and intelligent (smart) cooling strategies, with the smart approach activating water spraying only when the panel temperature exceeds a predefined threshold. This design aims to optimize thermal management while minimizing water consumption. The research investigates key performance parameters, including temperature, solar irradiation, electrical efficiency, and electrical power output under both continuous and smart cooling phases. In addition, economic and cost analyses were performed to evaluate the practical feasibility and cost-effectiveness of implementing such cooling systems in extreme environments.

By integrating adaptive thermal management with sustainable water use, this study offers a novel contribution to PV technology, providing a practical approach to improve energy efficiency, reduce operational costs, and enhance the economic viability of solar energy projects in arid regions. The findings also provide insights for the development and deployment of similar cooling strategies in other desert environments worldwide, addressing a critical challenge in PV performance optimization under extreme conditions.

2. Experimental setup

2.1. Climatic characteristics and geographical situation

This investigation was carried out in the city of Ouargla, located in the northeastern Algerian desert (31°52′ to 32°30′ N, 4°27′ to 5°26′ E) at an average elevation of 134 m, covering an area of 163,230 km^2 (Fig. 2). Ouargla's climate is characterized by arid desert conditions, marked by sporadic and limited rainfall, dryness, high temperatures, and winds dominated by hot, dry air currents. Furthermore, the region records one of the highest annual average solar radiation levels in the world, making it an ideal location for renewable energy research.

Table. 2
Technical Specifications of the Photovoltaic Modules (ZGE_FM72_390).

Parameter	Specification
Module type	Monocrystalline
Maximum power (W)	390 W
Maximum current (A)	9.53 A
Maximum voltage (V)	41 V
Dimension	1967x992x40 mm
Weight	23.8 Kg
Temperature coefficient of efficiency	–0.39% per °C

Fig. 3 illustrates the meteorological characteristics of Ouargla from 2013 to 2023. The city is characterized by a high solar radiation, particularly in summer (Fig. 3.a). Temperatures can exceed 50 °C in summer, while they are below 22 °C in winter. The highest wind speeds occur during April and May, reaching around 5.8 m/s, whereas the lowest winds are reported in December and January, averaging about 3.5 m/s. Fig. 3.b shows humidity levels in winter, reaching approximately 50% in December. Humidity gradually declines throughout spring and summer, reaching a minimum of about 13% in July and August before rising again in autumn.

2.2. Description of the photovoltaic thermal (PV/T) cooling system

To enhance the efficiency of photovoltaic panels, a water-based cooling system was developed, as illustrated in Fig. 4. The experimental setup included two identical monocrystalline silicon photovoltaic panels (ZGE_FM72_390) from Zergoune Green Energy Company, installed at a 31° tilt facing south (the optimum angle for Ouargla city) [1], with the specifications listed in Table 2. Water was pumped from the storage tank at a flow rate of 3.5 L/min through a perforated PVC pipe (105 mm in length and 22 mm in internal diameter) fitted with nine uniformly spaced outlets, each 3 mm in diameter and inclined at an angle of approximately 40°. The pipe was mounted along the upper edge of the photovoltaic panel to ensure a uniform distribution of cooling water over the front surface. The first panel, Panel A, was cooled using

Table 3
Specifications of Measurement Devices.

Measuring value	Instrument and model	Device properties
Current and Voltage	Multimeter GDM-356	voltage with accuracy about ±0.8% and current with accuracy about ±0.5%,
Temperature	Digital thermometer RDXL4SD	Temperature range − 199.9–850 °C, device accuracy ±2%.
Solar radiation	Pyranometer Ruby Electronics	Solar irradiation range 0–1999 W/m^2, device accuracy ±8%

two methods: continuous and intelligent water spraying, while the second panel, Panel B, served as a reference. The water was repurposed to irrigate green spaces after serving its cooling function, contributing to sustainable resource use. The experiments were conducted from June 9 to July 4, 2024, to assess the impact of the cooling methods on power generation and overall system performance efficiency.

2.3. Instrumentation

A digital multimeter (GDM-356) was used to measure voltage and current. To safeguard the inputs of the interface board, two rheostats (Psy-Langlois) were incorporated, each rated at 320 W, 600 V, 5.7 A, with a resistance range of 0 to 10 Ω. A solar radiation meter (Ruby Electronics) was employed to assess the amount of solar energy reaching a specified surface. A digital thermometer (RDXL4SD) with an accuracy of ±0.5% was utilized to measure both the ambient temperature and the front and back surface temperatures of the PV panel. The solar charge controller (EASUN POWER) implemented in the system operates at a nominal voltage of 12 V/24 V, with a nominal current of 100 A, a maximum PV voltage of 50 V, and a peak PV input power of 1300 W (12 V) or 2600 W (24 V). The battery (Leoch) has a capacity of 12 V 100 AH. The system included a pump with a maximum pressure of 0.48 MPa, a maximum flow rate of 3.5 L/min, a DC voltage of 12 V, and a maximum current of 2.04 A. An Arduino board and a relay were employed to control the pump. All measuring devices were calibrated, and Table 3 illustrates the specifications of the equipment used in this study. Data collection was conducted manually.

2.4. Experimental methodology

The experimental setup was located on the roof of the Renewable Energy Laboratory at Kasdi Merbah University, Ouargla. To ensure reliable results and a clear comparison, two identical monocrystalline solar panels of 390 W were used. Both units were oriented south with a fixed tilt angle of 31 degrees. One panel was connected to a water-cooling system (denoted as Panel A), while the second panel served as a reference (denoted as Panel B). Before each test, both panels were properly cleaned. The experiments were conducted in two phases: continuous and smart cooling.

- **Baseline Calibration Test**

Before implementing any cooling strategy, a baseline calibration test was conducted to assess potential intrinsic performance differences between the two PV modules. Both panels were operated simultaneously under identical outdoor conditions without any cooling applied. Solar irradiance, voltage, and current were recorded at 30-min intervals from 09:30 to 15:00. The results of this preliminary test confirmed the performance equivalence of the modules and established a reliable reference for evaluating the effects of the cooling techniques.

- **Configuration I: Continuous Cooling**

During the first phase, conducted on June 9, 10, and July 1, 2, 2024, the panel was equipped with a continuous and uninterrupted cooling system, as shown in Fig. 5.a. Voltage, solar radiation, current, ambient temperature, and the front and back surface temperatures of the two PV panels were recorded every 30 min from 8:30 AM to 4:00 PM.

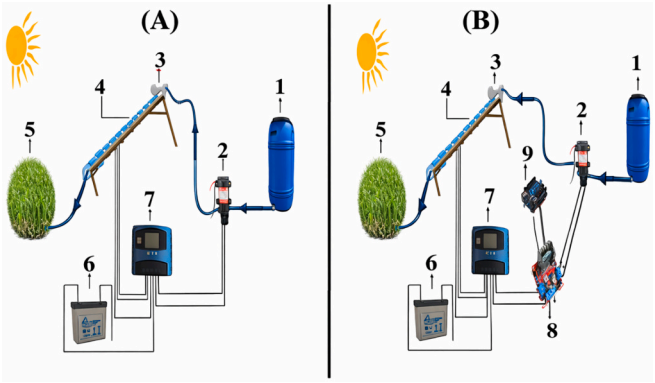

Fig. 5. Experimental Setup (a) Continuous, (b) Intelligent Cooling, (1) water tank, (2) pump, (3) Pipe outlets, (4) PV panel, (5) Green Space and Grass, (6) Battery, (7) Solar charge controller, (8) Relay module (9) Arduino. (For interpretation of the references to colour in this figure legend, the reader is referred to the web version of this article.)

- **Configuration II: Intelligent Cooling**

During the second phase (June 11, 12, and July 03, 04, 2024), the continuous cooling system was upgraded to an intelligent cooling system that incorporates an Arduino board, as shown in Fig. 5. b. In this phase, the photovoltaic module was equipped with an automated on–off smart cooling system designed to regulate the panel temperature based on real-time thermal feedback. The control unit comprised an Arduino microcontroller interfaced with a DHT22 digital temperature sensor fixed at the center of the panel's rear surface. The system was configured with a nominal set point of 40 °C and a hysteresis band of ±1.5 °C; the cooling process was activated when the rear surface temperature exceeded 41.5 °C and automatically deactivated once it dropped below 38.5 °C. A relay-driven pump circulated water from a storage tank and sprayed it uniformly over the front surface through a perforated PVC pipe fitted with outlets. Throughout the experiments, the thermal response, water consumption, and electrical output were continuously recorded to evaluate the system's cooling efficiency under varying operating conditions. The data was recorded every 30 min from 8:30 AM to 4:00 PM by measuring several parameters, including the front and rear surface temperatures of the PV panel, ambient temperature, solar irradiance, voltage, and current. Calculations of power output, efficiency for both the cooled and reference PV panels, and improvements in efficiency are performed using the equations provided by Abou Akrouch et al. [41].

$$P = Isc \times Voc \tag{1}$$

$$\eta = \left(\frac{P}{R \times S}\right) \times 100 \tag{2}$$

$$\eta_{improvement} = \left(\frac{\eta_{cooling} - \eta_{reference}}{\eta_{reference}}\right) \times 100 \tag{3}$$

2.5. Uncertainty analysis

To ensure the accuracy and validity of the experimental data, measurement uncertainties were analyzed using the instrument specifications in Table 3. The method of Kline and McClintock [42] was used to assess uncertainty propagation and evaluate the bias error of computed variables through the following equation:

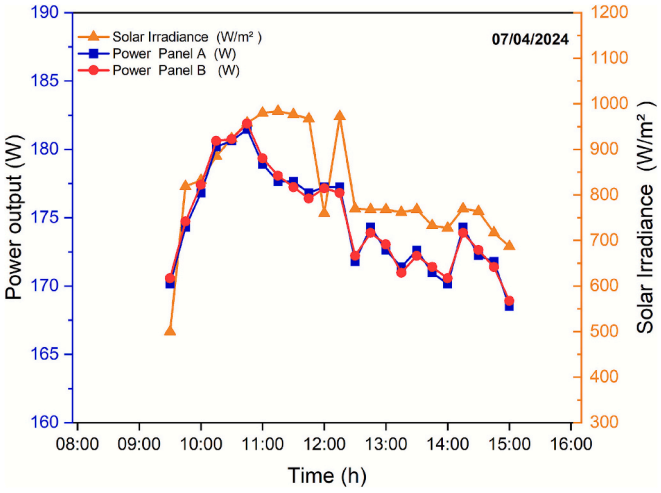

Fig. 6. Power and irradiance solar variations over time for **Baseline Calibration Test.**

$$w_Z = \sqrt{\sum_{i=1}^{n} \left(\frac{\partial Z}{\partial xi} w_{xi} \right)^2} \quad (4)$$

The errors in power and efficiency reduction were ± 0.94% and ± 0.136%, respectively.

3. Results and discussions

The experimental results are presented according to the cooling mode, namely continuous and smart cooling. Data was collected from 8:30 A.M. to 4:00 P.M. over eight days in June and July 2024, a period chosen for its peak solar irradiation and high temperatures, which varied between 128.8 W/m^2 and 982 W/m^2, and 30 °C to 45 °C, respectively.

- **Baseline Calibration Test**

Fig. 6 shows the variation of power output and solar irradiation over time for both PV modules. Both panels exhibited nearly identical power generation trends, with an average difference of 0.5% and deviations remaining within the measurement uncertainty of ±0.94%, confirming their initial equivalence. Minor fluctuations in solar irradiance between 11:45 and 14:00 were observed, attributed to transient cloud cover. These baseline measurements were subsequently used to normalize the results of the cooling experiments, ensuring that any observed performance improvements could be attributed solely to the applied cooling strategies.

- **Continuous cooling phase**

This phase took place over four sunny days (from June 9–10, 2024, to

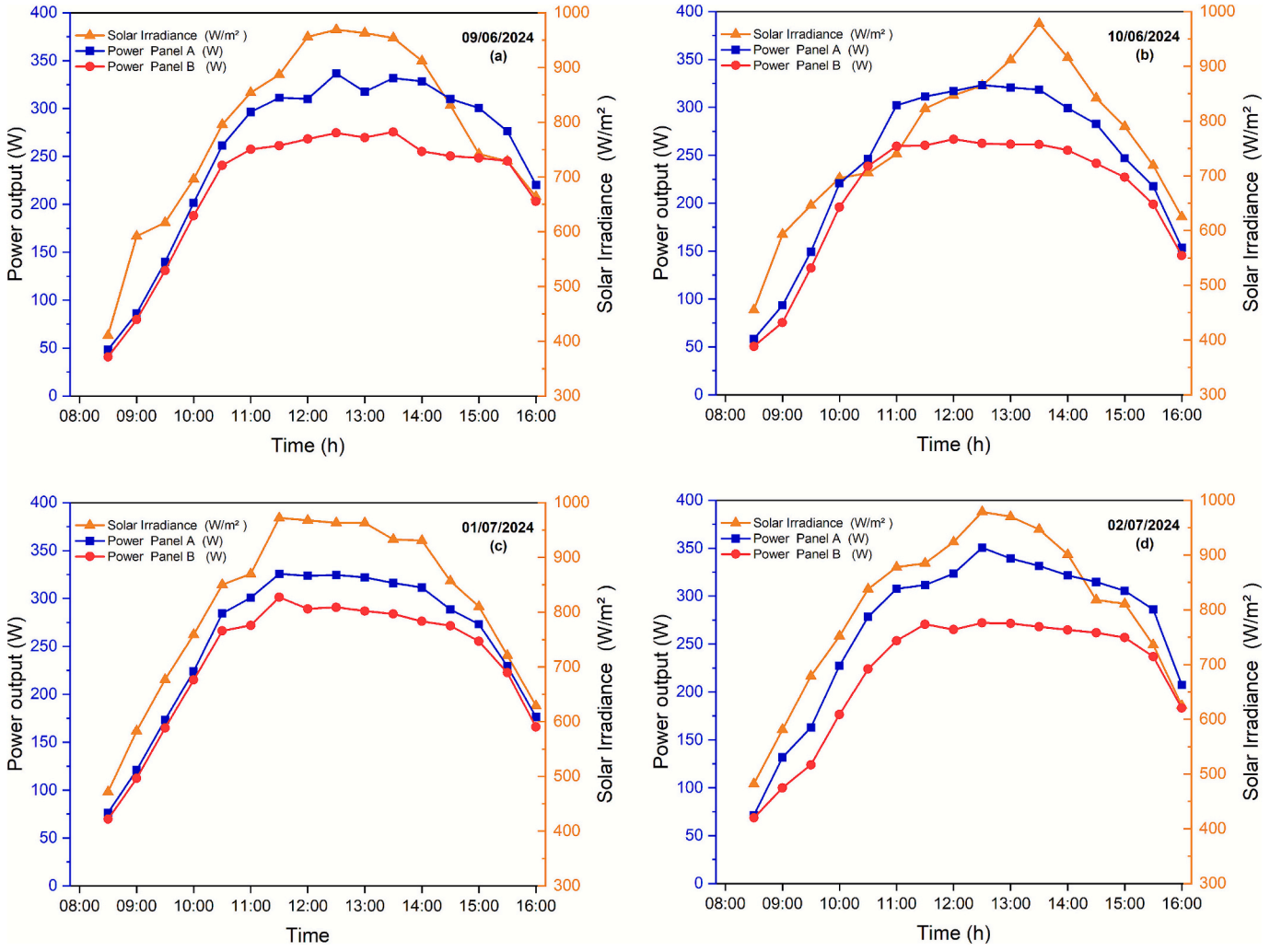

Fig. 7. Power and irradiance solar variations over time for continuous cooling.

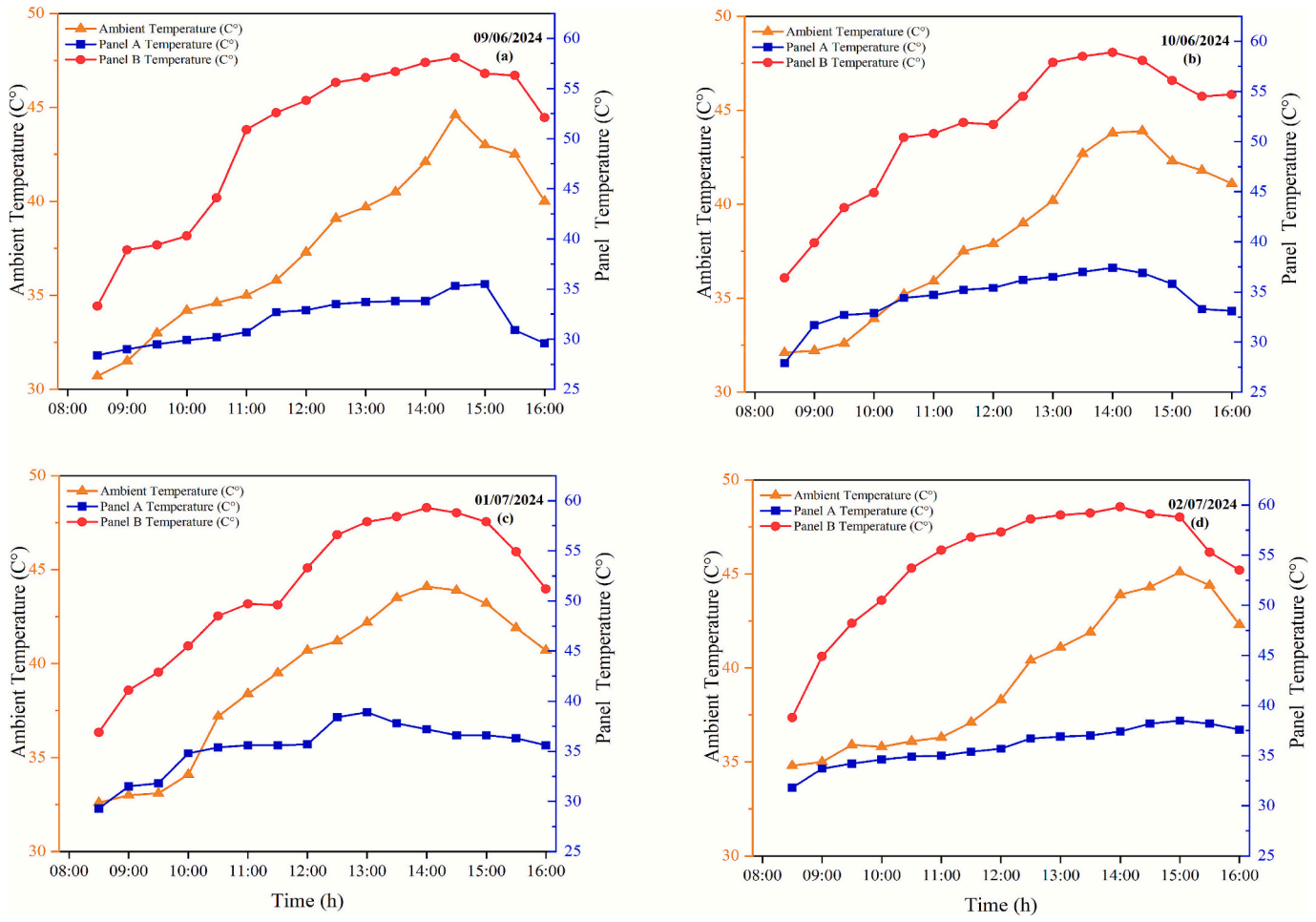

Fig. 8. Temperature variations over time for continuous cooling.

July 1–2, 2024). The cooling system operated continuously, with the pump running for an average of 450 min per day and a total water usage of about 1575 l.

Fig. 7 illustrates the variations in solar irradiation and power output over time. An increase in solar irradiation was recorded from 8:00 AM to 12:00 PM, reaching peak values around 12:30 PM. The maximum solar irradiation measured in Fig. 7a and b reached 969 W/m^2 and 979 W/m^2, respectively. In contrast, in Fig. 7c and d, the maximum values were 972 W/m^2 and 978 W/m^2, occurring at 11:30 AM and 1:30 PM, respectively.

During the period from 11:30 to 14:00, the maximum electrical power output from panel A (with a cooling system) over the four days, as shown in Figs. 7a, b, c, d, was 337 W, 323 W, 326 W, and 351 W, respectively. In contrast, panel B (without a cooling system) under the same conditions produced only 274 W, 262 W, 301 W, and 272 W, respectively. These results clearly indicate the positive effect of cooling on power generation.

Ambient temperature also showed an upward trend during this period, as shown in Figs. 8a, b, c, and d. The maximum ambient temperatures recorded were 44.6 °C, 43.9 °C, 44.1 °C, and 45.1 °C, respectively. Experimental data indicated that the surface temperature of the cooled PV panel consistently remained lower than that of the uncooled panel. The maximum temperature difference between cooled and uncooled panels during the period from 13:30 to 14:30 was 23.8 °C, 21.5 °C, 22.2 °C, and 22.4 °C, as shown in Figs. 9a, b, c, and d, respectively.

- **Smart cooling phase**

During the smart cooling phase, tests were conducted on June 11–12 and July 3–4, 2024. The system utilized temperature readings from the back of the PV panel; once it reached 40 °C, the Arduino controller automatically activated the pump to begin spraying water. On average, the pump operated for about 125 min per day, using a total of 437 l of water over all test days. Compared to continuous cooling, this approach achieved an 84% reduction in water usage. Fig. 9 presents the variations in power generation and solar irradiation over time during the smart cooling process. The figure shows an increase in solar irradiation from 8:30 AM to 1:00 PM, reaching its peak values. The maximum value of 960 W/m^2 was recorded at 1:00 PM in Fig. 9.a, while Fig. 9.b recorded a maximum value of 982 W/m^2 at 1:30 PM. The maximum values of 955 W/m^2 and 961 W/m^2 were respectively recorded at 12:30 PM (Figs. 9.c and 9.d).

It was observed that with water spray cooling, the power output was higher compared to the non-cooled panel. During the period from 11:30 AM to 1:30 PM, the maximum power recorded, in Figs. 9.a, b, c, and d, was 328 W, 326 W, 357 W, and 341 W for the cooled panel, respectively, while it was 294 W, 251 W, 300 W, and 285 W for the non-cooled panel. Fluctuations were noted, especially in Fig. 10b, where a decrease in power generation was recorded, reaching 288 W for the cooled panel and 216 W for the non-cooled panel at 1:00 PM. This change is attributed to a reduction in solar irradiation to approximately 734 W/m^2 due to the passage of clouds. This illustrates that the reflected radiation from passing clouds plays a crucial role in reducing the energy produced by the photovoltaic system.

Fig. 10 illustrates the temperature variations over time during the smart cooling process. The experimental results recorded with the smart

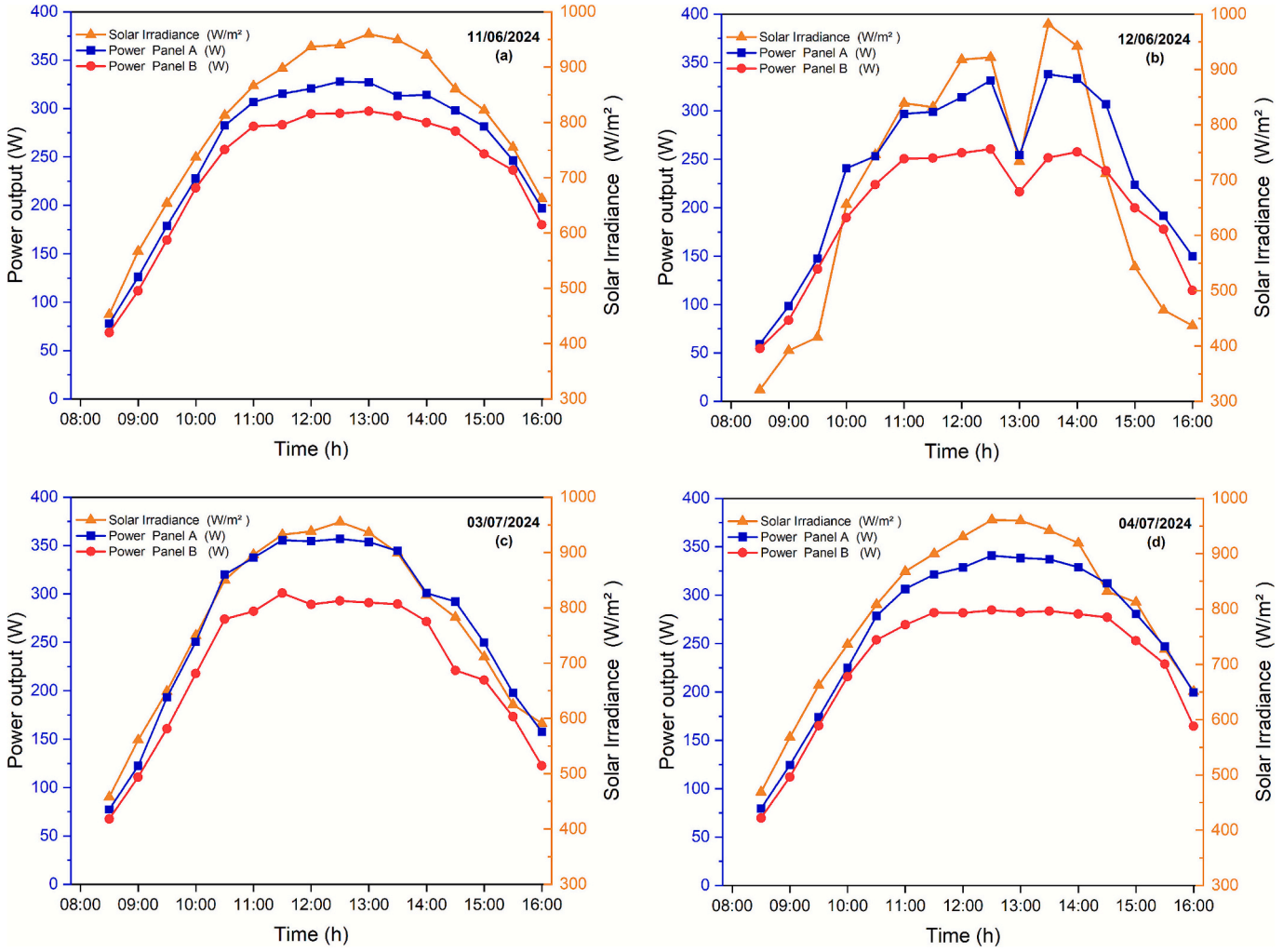

Fig. 9. Power and irradiance solar variations over time for smart cooling.

cooling system indicate that the temperature differences between the cooled and non-cooled panels in Fig. 10a, b, c, and d were 20.7 °C, 21 °C, 14.8 °C, and 19.1 °C, respectively. As shown in Fig. 10c, the temperature difference of 14.8 °C on July 3, 2024, can be explained by the fact that the maximum ambient temperature on this day was 38 °C lower than on other test days.

The performance of the continuous and intelligent cooling modes is comparable for power output; nevertheless, the intelligent mode has clear operating benefits such as water conservation and more effective use of pump power. Table 4 lists the mean temperatures, efficiency of the photovoltaic panel, consumption of water, and the running time of the pump for both intelligent and continuous cooling methods. From the data obtained, there is a marginal increase in efficiency for the intelligent cooling method, which may vary based on the intensity of solar irradiation available during the testing period. Smart cooling consumes less water with improved cooling effects. Additionally, the running time of the pump is shorter with reduced power consumption; this could have increased the durability of the pump. Also, the use of water has two benefits in cooling as well as cleaning the surfaces of the photovoltaic panel, thus combating efficiency reduction caused by the accumulation of dust.

- **Comparison of Photovoltaic Cooling Efficiency Across Studies**

The cooling results show that both proposed cooling modes are practical and competitive compared to recent published studies (Table 5). The continuous cooling system reached an efficiency of 15.45%, while the Smart cooling system achieved a slightly higher value of 15.50%. The results are closely consistent with those published by Nižetić et al. [15], who achieved 15.42% improvement in efficiency with front-side spraying and 15.59% with back-side spraying. The results of this study indicate better performance compared to evaporative cooling (15% efficiency reported by Yang et al. [27]) and back-side water pipe cooling (13.79% by Shalaby et al. [32]). While higher efficiency levels were achieved with more complex techniques like immersed cooling, which reached 17.7% and 17.8% according to Zubeer and Ali [18] and Saurabh Mehrotra et al. [33], respectively, these systems often require more complex setups and frequent maintenance. In contrast, the cooling methods tested here strike a good balance between performance and simplicity. They offer a significant improvement in efficiency while remaining easy to implement and maintain, which is especially valuable in real-world conditions where budget, maintenance, and water use are crucial concerns. The smart cooling method has potential for further enhancement through advanced control systems, sensor-based feedback, or even machine learning, aimed at increasing both energy output and resource utilization efficiency.

- **Cost Analysis**

Estimating the cost of energy production necessitates analyzing the initial economic investment of the proposed systems. To this end, an economic evaluation was conducted for a conventional PV system as

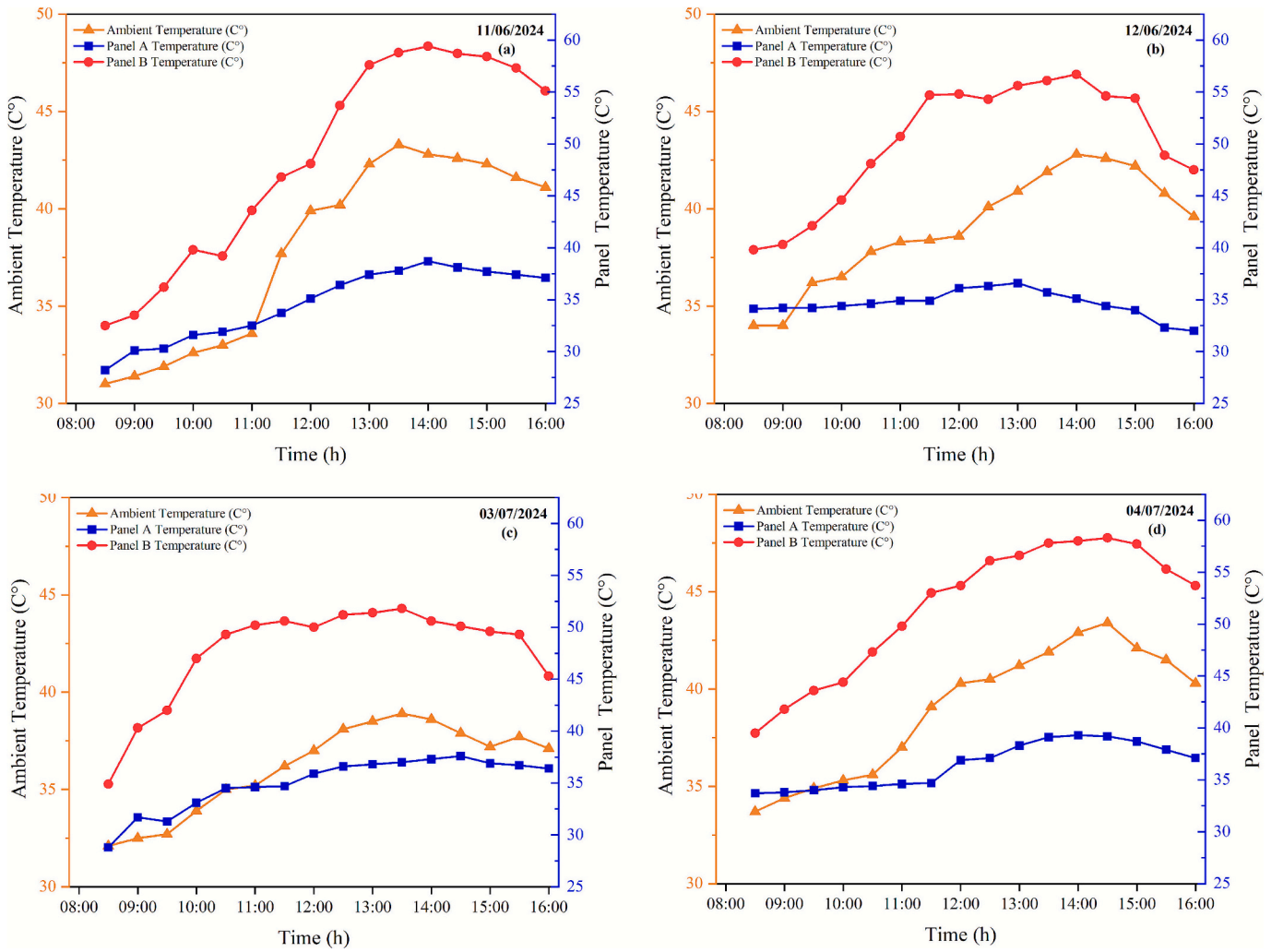

Fig. 10. Temperature variations over time for smart cooling.

Table 4
Comparison between intelligent and continuous cooling configurations.

Cooling Mode	Average Cooling Efficiency (%)	Average Water Consumption (L per kWh)	Daily Pump Operating Duration (min)	Pump Power Consumption (W)	Average PV Module Temperature (°C)
Continuous cooling	15.44	391.95	450	183.6	34.41
		63.86	75	30.6	35.16
Intelligent cooling	15.5				

well as for modified PV systems that incorporate two water spray cooling techniques: continuous and smart cooling. Table 6 provides a comparison of the component costs utilized in the smart cooling system, the continuous cooling system, and the conventional system, respectively.

To evaluate the economic performance of various PV system configurations, a standard cost analysis was performed over a system lifespan of n years, with an annual interest rate of i. The capital cost (CS) represents the initial investment needed for system installation. Table 7 presents the equations (Dawood et al. [43]), used to estimate the annual cost per watt of power productivity (CPW).

The annual operating cost includes the electrical energy consumption of the water pump, calculated based on its rated power and daily operating duration for each cooling strategy. The results clearly demonstrate that the Smart Cooling system achieves the lowest annual cost per watt of power produced, at 0.07020 €/W. This represents a cost advantage over both continuous cooling (0.07514 €/W) and the no-cooling configuration (0.07135 €/W), highlighting the economic efficiency of the proposed Smart Cooling approach for photovoltaic panels in desert climates.

4. Conclusion

The extremely hot and arid environment of Algeria's desert areas is an important limiting factor for the efficiency and performance of photovoltaic (PV) modules. Water spray cooling with a continuous process, as well as intelligent control, is shown in this study to be capable of reducing module temperatures and improving power generation. A continuous process increases power generation from 272.1 W to 350.5 W with a corresponding reduction in module temperature from

Table 5
Comparative Cooling Efficiency of the Proposed PVT Systems against previous Methods in the Literature.

References	Cooling Method	Cooling Efficiency
Nižetić et al. [15]	Front Surface spray	15.42%
Nižetić et al. [15]	Back surface spray	15.59%
Opeyeolu et Moyahabo [17]	Front Surface spray	16.65%
Zubeer and Ali. [18]	Front Surface spray	17.7%
Raju et al. [19]	Front Surface spray	15.73%
Hassan et al. [21]	Front Surface spray	14.8%
Yang et al. [27]	Evaporative	15%
Mostakim and Khodadad [25]	Front spray	16.78%
Shalaby.et al. [32]	Back Water pipe	13.79%.
Saurabh Mehrotra et al. [33]	Immersed	17.8%
Sivakumar et al. [34]	Immersed	15.54%
Actual Study: Continuous Cooling	Front spray	15.44%
Actual Study: Smart Cooling	Front spray	15.50%

Table 6
Cost of components.

Components	Cost of components €		
	Smart cooling	Continuous cooling	Without cooling
Solar PV panel	102 €	102 €	102 €
Battery	180 €	180 €	180 €
Solar charge controller	18 €	18 €	18 €
Connectors	1 €	1 €	1€
Pump	13 €	13 €	/
Tank	10 €	10 €	/
Arduino with accessories	8 €	/	/
DHT22 temperature sensor	1 €	/	/
Pipe sprayed	1 €	1€	/
Water pipe size 8 mm^2	2 €	2 €	/
Water pipe size 25 mm^2	13 €	13 €	/
Accessories	2 €	2 €	/
Total	**350 €**	**342 €**	**301 EURO**

58.6 °C to 36.7 °C. Intelligent control increases power generation from 251 W to 337 W while lowering module temperature from 56.1°C to 35.7 °C. Analysis of performance shows that while continuous cooling is more efficient with a cooling efficiency of 15.44%, water use is excessively high at 391.95 L/kWh with longer operating time for the pump of 450 min/day and higher power use of 183.6 W. Intelligent methods are relatively equal in cooling efficiency at 15.5% but with greatly decreased water use of 63.86 L/kWh, shorter operating time of 75 min/day for the pump, and lower power of 30.6 W. Regarding costs, intelligent cooling is decidedly cheaper with yearly electricity expenses of 0.07020 €/W than continuous processes at 0.07514 €/W and non-cooling systems at 0.07135 €/W. It can be said that both cooling systems are effective in countering the negative impact of high temperature on the efficiency of solar cells in PV systems. Though absolute power may be higher in the case of continuous cooling, the benefits of intelligent cooling in terms of cost, consumption, and use of water make it the preferred choice in desert conditions.

5. Future Work

Future research will investigate the role of additional environmental parameters such as wind speed and humidity to further improve cooling strategies. Moreover, analysis of advanced cooling techniques such as nanofluid cooling and further optimizing the mass flow rate based on varying environmental settings will be vital to further boost power generation and sustain efficient operation of PV systems in a desert environment.

Table 7
Economic analysis results.

Parameter	Equation	Smart Cooling	Continuous Cooling	Without Cooling
The capital cost (CS)	/	350	342	301
Interest per year i, (%)	/	12	12	12
life time (year)	/	25	25	25
Salvage value (Sa)	$Sa = 0.2 \times CS$	70	68.4	60.2
Capital Recovery Factor (CRF)	$CRF = \frac{i(i+1)^n}{(i+1)^n - 1}$	0.1275	0.1275	0.1275
Sinking fund factor (SFF)	$SFF = \frac{i}{(1+i)^n - 1}$	0.0075	0.0075	0.0075
Fixed annual cost (FAC)	FAC = CRF × CS	44.625	43.605	38.3775
Annual operating and maintenance cost (AMC)	AMC =0.15 × FAC	6.69375	6.54075	5.756625
Annual pump energy cost (APC)	$APC = P_p \times 365 \times C_e$	0.4579	2.7475	0
Annual salvage value (ASV)	ASV=SFF × Sa	0.525	0.513	0.4515
Annual power productivity (AP), W	AP = MPW × t × 365 × 25	730.03059	697.03636	612,224.6993
Total annual cost (TAC)	TAC = FAC + AMC + APC –ASV	51.25165	52.380324	43.682625
Annual cost per 1 W of power productivity (CPW)	$CRF = \frac{TAC}{AP}$	0.07020	0.07514	0.07135

Declaration of competing interest

The authors declare that they have no known competing financial interests or personal relationships that could have appeared to influence the work reported in this paper.

Data availability

Data will be made available on request.

References

[1] Z. Chaich, D. Belatrache, A. Dobbi, S. Hadjadj, Experimental analysis of dust's impact on solar photovoltaic system efficiency in arid environments: a case study in southern Algeria, Environ. Sci. Pollut. Res. 31 (2024) 53315–53328, https://doi.org/10.1007/s11356-024-34776-8.
[2] S.K. Marudaipillai, B. Karuppudayar Ramaraj, R.K. Kottala, M. Lakshmanan, Experimental study on thermal management and performance improvement of solar PV panel cooling using form stable phase change material, Energy Sources Part Recovery Util Environ Eff 45 (2023) 160–177, https://doi.org/10.1080/15567036.2020.1806409.
[3] D. Govindasamy, A. Kumar, Experimental analysis of solar panel efficiency improvement with composite phase change materials, Renew. Energy 212 (2023) 175–184, https://doi.org/10.1016/j.renene.2023.05.028.
[4] Z. Li, T. Ma, J. Zhao, A. Song, Y. Cheng, Experimental study and performance analysis on solar photovoltaic panel integrated with phase change material, Energy 178 (2019) 471–486, https://doi.org/10.1016/j.energy.2019.04.166.
[5] A. Al Miaari, H.M. Ali, Technical method in passive cooling for photovoltaic panels using phase change material, Case Stud. Therm. Eng. 49 (2023) 103283, https://doi.org/10.1016/j.csite.2023.103283.
[6] A. Hussien, A. Eltayesh, H.M. El-Batsh, Experimental and numerical investigation for PV cooling by forced convection, Alex. Eng. J. 64 (2023) 427–440, https://doi.org/10.1016/j.aej.2022.09.006.
[7] R. Mazón-Hernández, J.R. García-Cascales, F. Vera-García, A.S. Káiser, B. Zamora, Improving the electrical parameters of a photovoltaic panel by means of an induced or forced air stream, Int J Photoenergy 2013 (2013) 830968, https://doi.org/10.1155/2013/830968.

[8] King M, Li D, Dooner M, Ghosh S, Roy JN, Chakraborty C, et al. Mathematical modelling of a system for solar PV efficiency improvement using compressed air for panel cleaning and cooling. Energies 2021;14:4072. Doi: https://doi.org/10.3390/en14144072.
[9] D. Nebbali, R. Nebbali, A. Ouibrahim, Improving photovoltaic panel performance via an autonomous air cooling system – experimental and numerical simulations, Int J Ambient Energy 41 (2020) 1387–1403, https://doi.org/10.1080/01430750.2018.1517670.
[10] N.A.S. Elminshawy, A.M.I. Mohamed, K. Morad, Y. Elhenawy, A.A. Alrobaian, Performance of PV panel coupled with geothermal air cooling system subjected to hot climatic, Appl. Therm. Eng. 148 (2019) 1–9, https://doi.org/10.1016/j.applthermaleng.2018.11.027.
[11] G.M. Tina, M. Rosa-Clot, P. Rosa-Clot, P.F. Scandura, Optical and thermal behavior of submerged photovoltaic solar panel: SP2, Energy 39 (2012) 17–26, https://doi.org/10.1016/j.energy.2011.08.053.
[12] M. Nateqi, M. Rajabi Zargarabadi, R. Rafee, Experimental investigations of spray flow rate and angle in enhancing the performance of PV panels by steady and pulsating water spray system, SN Appl. Sci. 3 (2021) 1–13, https://doi.org/10.1007/s42452-021-04169-4.
[13] H.A. Hasan, J.S. Sherza, J.M. Mahdi, H. Togun, A.M. Abed, R.K. Ibrahim, et al., Experimental evaluation of the thermoelectrical performance of photovoltaic-thermal systems with a water-cooled heat sink, Sustainability 14 (2022) 10231, https://doi.org/10.3390/su141610231.
[14] M. Alktranee, P. Bencs, Effect of evaporative cooling on photovoltaic module performance, Process Integr Optim Sustain 6 (2022) 921–930, https://doi.org/10.1007/s41660-022-00268-w.
[15] S. Nižetić, D. Čoko, A. Yadav, F. Grubišić-Čabo, Water spray cooling technique applied on a photovoltaic panel: the performance response, Energy Convers. Manag. 108 (2016) 287–296, https://doi.org/10.1016/j.enconman.2015.10.079.
[16] P. Bevilacqua, R. Bruno, N. Arcuri, Comparing the performances of different cooling strategies to increase photovoltaic electric performance in different meteorological conditions, Energy 195 (2020) 116950, https://doi.org/10.1016/j.energy.2020.116950.
[17] O.T. Laseinde, M.D. Ramere, Efficiency improvement in polycrystalline solar panel using thermal control water spraying cooling, Procedia Comput Sci 180 (2021) 239–248, https://doi.org/10.1016/j.procs.2021.01.161.
[18] S.A. Zubeer, O.M. Ali, Experimental and numerical study of low concentration and water-cooling effect on PV module performance, Case Stud. Therm. Eng. 34 (2022) 102007, https://doi.org/10.1016/j.csite.2022.102007.
[19] M. Raju, R.N. Sarma, A. Suryan, P.P. Nair, S. Nižetić, Investigation of optimal water utilization for water spray cooled photovoltaic panel: a three-dimensional computational study, Sustain. Energy Technol. Assess. 51 (2022) 101975, https://doi.org/10.1016/j.seta.2022.101975.
[20] S.A. Zubeer, O.M. Ali, Performance analysis and electrical production of photovoltaic modules using active cooling system and reflectors, Ain Shams Eng. J. 12 (2021) 2009–2016, https://doi.org/10.1016/j.asej.2020.09.022.
[21] A. Hassan, S. Abbas, S. Yousuf, F. Abbas, N.M. Amin, S. Ali, et al., An experimental and numerical study on the impact of various parameters in improving the heat transfer performance characteristics of a water based photovoltaic thermal system, Renew. Energy 202 (2023) 499–512, https://doi.org/10.1016/j.renene.2022.11.087.
[22] A. Bai, J. Popp, P. Balogh, Z. Gabnai, B. Pályi, I. Farkas, et al., Technical and economic effects of cooling of monocrystalline photovoltaic modules under Hungarian conditions, Renew. Sust. Energ. Rev. 60 (2016) 1086–1099, https://doi.org/10.1016/j.rser.2016.02.003.
[23] A. Hadipour, M. Rajabi Zargarabadi, S. Rashidi, An efficient pulsed- spray water cooling system for photovoltaic panels: experimental study and cost analysis, Renew. Energy 164 (2021) 867–875, https://doi.org/10.1016/j.renene.2020.09.021.
[24] Q. Zhang, S. He, T. Song, M. Wang, Z. Liu, J. Zhao, et al., Modeling of a PV system by a back-mounted spray cooling section for performance improvement, Appl. Energy 332 (2023) 120532, https://doi.org/10.1016/j.apenergy.2022.120532.
[25] K. Mostakim, MdR Akbar, MdA Islam, MdK Islam, Integrated photovoltaic-thermal system utilizing front surface water cooling technique: an experimental performance response, Heliyon 10 (2024) e25300, https://doi.org/10.1016/j.heliyon.2024.e25300.
[26] H. Necib, H. Kadi, D. Belatrache, Y.B. Hammou, Experimental evaluation of water cooling effects on photovoltaic module performance in a hot climate, Int. J. Energy Water Resour. 9 (2025) 1467–1483, https://doi.org/10.1007/s42108-025-00346-y.
[27] C. Yang, J. Lin, F. Miksik, T. Miyazaki, K. Thu, Dew-point evaporative cooling of PV panels for improved performance, Appl. Therm. Eng. 236 (2024) 121695, https://doi.org/10.1016/j.applthermaleng.2023.121695.
[28] T. Chea, T. Deethayat, T. Kiatsiriroat, A. Asanakham, Experiment and model of a photovoltaic module with evaporative cooling, Results Eng. 19 (2023) 101290, https://doi.org/10.1016/j.rineng.2023.101290.
[29] M. Alktranee, B. Péter, Energy and exergy analysis for photovoltaic modules cooled by evaporative cooling techniques, Energy Rep. 9 (2023) 122–132, https://doi.org/10.1016/j.egyr.2022.11.177.
[30] Y. Zhang, C. Shen, C. Zhang, J. Pu, Q. Yang, C. Sun, A novel porous channel to optimize the cooling performance of PV modules, Energy Built Environ 3 (2022) 210–225, https://doi.org/10.1016/j.enbenv.2021.01.003.
[31] A.A.B. Baloch, H.M.S. Bahaidarah, P. Gandhidasan, F.A. Al-Sulaiman, Experimental and numerical performance analysis of a converging channel heat exchanger for PV cooling, Energy Convers. Manag. 103 (2015) 14–27, https://doi.org/10.1016/j.enconman.2015.06.018.
[32] S.M. Shalaby, M.K. Elfakharany, B.M. Moharram, H.F. Abosheiasha, Experimental study on the performance of PV with water cooling, Energy Rep. 8 (2022) 957–961, https://doi.org/10.1016/j.egyr.2021.11.155.
[33] Y. El Alami, E. Baghaz, R. Nasrin, K. Haboubi, M. Benhmida, A. Ibrahim, Integrated sustainability and 4E analysis of hybrid nanofluid featured PVT systems incorporating diverse backsheets, Appl. Therm. Eng. 284 (2026) 129147, https://doi.org/10.1016/j.applthermaleng.2025.129147.
[34] Y. El Alami, E. Baghaz, R. Nasrin, S. Padmanaban, M. Louzazni, Numerical approach of an advanced hybrid photovoltaic thermal system based on exergy, energy, enviro-economic, and sustainability factors, Results Eng. 27 (2025) 106342, https://doi.org/10.1016/j.rineng.2025.106342.
[35] Y. El Alami, H. El Achouby, E. Baghaz, C. Hajjaj, R. Nasrin, An innovative photovoltaic thermal system with direct water-cell contact: energy, exergy, and sustainability analysis, Sol. Energy 300 (2025) 113827.
[36] Y. El Alami, E. Baghaz, R. Nasrin, F. Chanaa, R. Bendaoud, S. Padmanaban, M. Louzazni, Experimental-numerical comparative study of performance and cost-effectiveness of partially- and fully-cooled photovoltaic thermal systems, Case Stud. Thermal Eng. 73 (2025) 106660, https://doi.org/10.1016/j.csite.2025.106660.
[37] S. Mehrotra, P. Rawat, M. Debbarma, Performance of a Solar Panel with Water Immersion Cooling Technique, 2014.
[38] B. Sivakumar, S. Navakrishnan, M.R. Cibi, R. Senthil, Experimental study on the electrical performance of a solar photovoltaic panel by water immersion, Environ. Sci. Pollut. Res. 28 (2021) 42981–42989, https://doi.org/10.1007/s11356-021-15228-z.
[39] Solar resource maps & GIS data for 200+ countries | Solargis. https://solargis.com/resources/free-maps-and-gis-data?locality=algeria, 2026 accessed August 3, 2025.
[40] J. Remund, S. Müller, M. Schmutz, P. Graf, Meteonorm version 8. METEOTEST Www Meteotest Com, 2020.
[41] M.A. Akrouch, K. Chahine, J. Faraj, F. Hachem, C. Castelain, M. Khaled, Advancements in cooling techniques for enhanced efficiency of solar photovoltaic panels: a detailed comprehensive review and innovative classification, Energy Built Environ 6 (2025) 248–276, https://doi.org/10.1016/j.enbenv.2023.11.002.
[42] S.J. Kline, F.A. McClintock, Describing uncertainties in single-sample experiments, ASME Mech. Eng. 75 (1953).
[43] M.M. Khairat Dawood, A.I. Shehata, A.S. Shehata, A.E. Kabeel, K. Ramzy, A. M. Abdalla, et al., Experimental investigation of a stepped solar still employing a phase change material, a conical tank, and a solar dish, Int. J. Energy Res. 46 (2022) 16762–16776, https://doi.org/10.1002/er.8337.